Thermo- and Mechano-triggered Luminescence ON/OFF Switching by Supercooled Liquid/Crystal Transition of Platinum(II) Complex Thin Films

Masaki Yoshida,*,+[a] Verner Sääsk,+[a,b] Daisuke Saito,[a,c] Nobutaka Yoshimura,[a] Junichi Takayama,[d] Satoshi Hiura,[d] Akihiro Murayama,[d] Kaija Põhako-Esko,[b] Atsushi Kobayashi,[a] and Masako Kato*[a,c]

[a] Dr. M. Yoshida,+ V. Sääsk,+ D. Saito, N. Yoshimura, Dr. A. Kobayashi, Prof. Dr. M. Kato
Department of Chemistry, Faculty of Science, Hokkaido University
North-10 West-8, Kita-ku, Sapporo, Hokkaido 060-0810 (Japan)
E-mail: myoshida@sci.hokudai.ac.jp, katom@kwansei.ac.jp
[b] V. Sääsk,+ Prof. Dr. K. Põhako-Esko
Institute of Technology, University of Tartu
Nooruse 1, Tartu 50411 (Estonia)
[c] D. Saito, Prof. Dr. M. Kato
Department of Applied Chemistry for Environment, School of Biological and Environmental Sciences, Kwansei Gakuin University
2-1 Gakuen, Sanda, Hyogo 669-1337 (Japan)
[d] J. Takayama, Dr. S. Hiura, Prof. Dr. A. Murayama
Faculty of Information Science and Technology, Hokkaido University
North-14 West-9, Kita-ku, Sapporo, Hokkaido 060-0814 (Japan)
[+] Co-first authors.

Supporting information for this article is given via a link at the end of the document.

Abstract: Trihexyltetradecylphosphonium ($P_{6,6,6,14}$) salts of luminescent anionic Pt(II) complexes, $(P_{6,6,6,14})[PtX_2(ppy)]$ (X = Cl^-, Br^-; ppy = 2-phenylpyridinate) were synthesized and photofunctional thin films with crystal/liquid bi-stability were fabricated. In particular, the chloride complex provided a thin film exhibiting thermo- and mechano-triggered luminescence ON/OFF switching at ambient temperature, which was based on the control of the supercooled liquid phase and bright luminescent crystalline phase. The photophysical properties of the complexes were investigated and compared with those of the bromide complex and tetra(*n*-butyl)ammonium salts of the complexes. Furthermore, detailed photophysical analysis revealed a large contribution of the charge-transfer character to the ligand-centered $^3\pi\pi^*$ excited state, which resulted in intense phosphorescence in the crystal and high-contrast luminescence ON/OFF by the phase transition of the chloride complex.

Introduction

Phosphorescent transition-metal complexes, such as Pt(II), Ir(III), and Ru(II) complexes, have recently attracted growing attention because of not only their excellent photophysical properties and high quantum efficiencies,[1,2] but also as stimuli-responsive properties to mechanical forces, vapor, and temperature changes.[3] In particular, the fabrication of polycrystalline thin films of phosphorescent transition-metal complexes enables a wide range of optical/optoelectronic applications, including light-emitting devices[4] and sensors that respond rapidly to gases/vapors.[5] To fabricate such photofunctional polycrystalline thin films, the vacuum deposition process or the solution process by spin-coating are widely used, but the former requires high temperature and high vacuum, whereas the latter has difficulties in controlling the uniformity and/or amount of loading. Although there have been recent reports on the fabrication of photofunctional thin films of nanocrystals of transition-metal complexes doped in polymers,[4c,5d] the fabrication of non-doped translucent thin films of phosphorescent metal complexes still remains a challenge. For the easy fabrication of such optical devices with large surface areas, it is a promising strategy to liquefy the luminophore.[6] The liquefication of phosphorescent metal complexes at ambient temperature (typically, below 100 °C) has mainly been reported for lanthanide(III) complexes,[7] and there are relatively few reports of liquescent and phosphorescent d-block metal complexes, including Cu(I), Au(I), and Ru(II) complexes.[8] We have recently succeeded in the liquefication of luminescent Pt(II) complexes showing obvious thermochromic luminescence.[9] However, most of them are difficult to crystallize at room temperature, and only a few of these liquids exhibit stimuli-responsiveness.[8f,h,9]

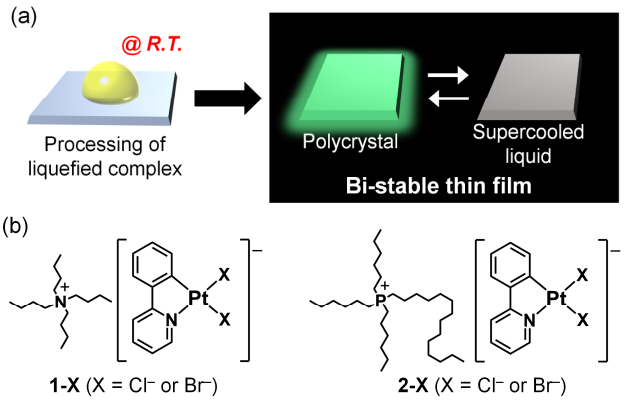

Scheme 1. (a) Schematic representation of the fabrication of a stimuli-responsive thin film using liquescent transition-metal complex. (b) Structural formulas of complexes.

In this context, crystal/liquid bi-stability (i.e., hysteretic crystallization/melting behavior)[10] would enable the easy fabrication of luminescent and stimuli-responsive crystalline films

at ambient temperature (Scheme 1(a)). To achieve such properties, we selected the trihexyltetradecylphosphonium ($P_{6,6,6,14}$) cation bearing asymmetric long alkyl chains. In addition to lowering the melting point, $P_{6,6,6,14}$ salts are also expected to crystallize gradually because of van der Waals interactions between the alkyl chains, resulting in the formation of a metastable supercooled liquid state.[11] As an anionic phosphor for the $P_{6,6,6,14}$ cation, $[PtX_2(ppy)]^-$ (X = Cl^- or Br^-, ppy = 2-phenylpyridinate) was selected because of its photophysical properties depending on the environment: $(Bu_4N)[PtCl_2(ppy)]$ (**1-Cl** in Scheme 1(b))[12] and derivatives[13] were reported to exhibit strong ligand-centered $^3\pi\pi^*$ emission in the crystal, whereas the emission was completely quenched in the fluid media. Thus, the highly contrasting luminescence behavior of $[PtCl_2(ppy)]^-$ motivated us to create a high-contrast luminescence ON/OFF switchable system coupled with the hysteretic phase transition.

Herein, we report thermo/mechano-responsive luminescent films based on $(P_{6,6,6,14})[PtX_2(ppy)]$ (**2-X** in Scheme 1(b); X = Cl^- or Br^-). **2-X** exhibited obvious luminescence in the crystal phase, and the emissions were completely quenched by melting. Importantly, **2-X** adopted a metastable supercooled ionic liquid phase that crystallized by mechanical stimulation, enabling the mechanostress-induced turn-on of luminescence at ambient temperature. In addition, by comparison with the corresponding Bu_4N^+ salts $(Bu_4N)[PtX_2(ppy)]$ (**1-X** in Scheme 1(b); X = Cl^- or Br^-), the unusually large contribution of the charge-transfer character to the $^3\pi\pi^*$ excited state of $[PtX_2(ppy)]^-$ ions was first revealed, which enables intense phosphorescence in the crystal and high-contrast luminescence ON/OFF behavior between the crystal and liquid phases. Thus, we realized the fabrication of a translucent non-doped film with high-contrast luminescence ON/OFF switching triggered by mechanostress.

Results and Discussion

Synthesis and Thermal Properties

New complex salts were successfully synthesized as yellow crystalline solids by the reaction of $[Pt_2(\mu\text{-}X)_2(ppy)_2]$ with $(Bu_4N)Br$ (for **1-Br**) or $(P_{6,6,6,14})X$ (for **2-X**) in dichloromethane (see Supporting Information for details), while **1-Cl** was synthesized according to a previously reported method.[14] X-ray crystallographic analysis of **1-Br** revealed that the Pt atom adopted a four-coordinated square-planar geometry (Figure S1), as typically observed for divalent platinum complexes. Although square-planar Pt(II) complexes tend to assemble based on Pt–Pt and/or π–π interactions,[3] bulky Bu_4N^+ cations prevent such interactions to afford the "discrete" nature.[2d,15] Likewise, the photophysical measurements indicated the discrete environments for all the Pt(II) complexes (not only **1-Cl** and **1-Br**, but also **2-Cl** and **2-Br**) in their crystal phases (*vide infra*), although it was difficult to conduct the X-ray crystallographic analysis of **2-Cl** and **2-Br**.

To investigate the phase transition behavior, differential scanning calorimetry (DSC) and differential thermal analysis (DTA) were performed, as summarized in Table 1. The DSC curves of **2-Cl** and **2-Br** (Figure 1(a,b)) in the first heating process displayed an endothermic peak at 326 K (**2-Cl**) and 325 K (**2-Br**), corresponding to the melting of complexes to form the ionic liquid phase. In the subsequent cooling process, no exothermic peaks appeared, and only a slight change in the baseline assignable to the glass transition at approximately T_g = 225 K (**2-Cl**) and 216 K (**2-Br**) were observed for both complexes (Figures 1(a,b) and S2). This result indicates that the cooling of melted **2-Cl** and **2-Br** resulted in a stable supercooled liquid phase. Indeed, variable-temperature powder X-ray diffraction (VT-PXRD) measurements (Figure 1(c,d)) revealed that the diffraction peaks of **2-Cl** and **2-Br** disappeared above 323 K, and the peaks did not recover even after cooling to 293 K. Importantly, the DSC curves in the second heating process displayed an exothermic peak at 308 K (**2-Cl**) and 282 K (**2-Br**), prior to the second melting at approximately 323 K. Therefore, the metastable supercooled liquids of **2-Cl** and **2-Br** thermally undergo crystallization at ambient temperature (i.e., cold crystallization).[7h,10,11,16] This thermal process was also confirmed by variable-temperature microscopic observations (Figure S3). In contrast, the melting points of **1-Cl**[17] and **1-Br** (T_m = 458 K and 443 K, respectively; Figure 1(e)) are significantly higher than those of **2-X**, indicating the importance of the low-symmetry of $P_{6,6,6,14}$ ions for lowering the melting point. Thus, we have succeeded in obtaining metastable supercooled ionic liquid phases for **2-Cl** and **2-Br** and thermal crystallization of their supercooled liquid phases using $P_{6,6,6,14}$ cations.

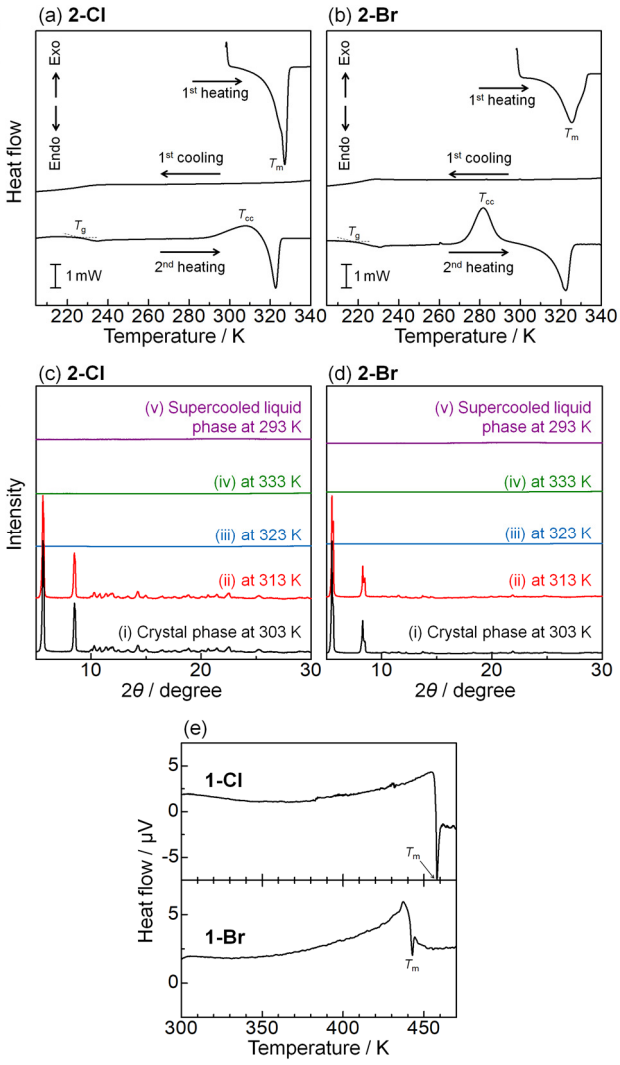

Figure 1. (a,b) DSC curves of (a) **2-Cl** and (b) **2-Br** (scan rate = 5 K/min) under N_2 flow. Magnified DSC curves around T_g are shown in Figure S2. (c,d) VT-PXRD patterns of (c) **2-Cl** and (d) **2-Br**. (e) DTA curves of **1-Cl** (top) and **1-Br** (bottom) (scan rate = 2 K/min) under Ar flow.

Table 1. Thermal properties of complexes.

	T_m[a] / K	T_g[b] / K	T_{cc}[c] / K
1-Cl	458[d]	–	–
2-Cl	326	225	308
1-Br	443	–	–
2-Br	325	216	282

[a] Melting points. [b] Glass transition temperature. [c] Cold crystallization temperature. [d] Almost identical to the value in the literature (461 K).[17]

Photophysical Properties

To confirm the absence of electronic interactions between the complexes in the crystal, UV/Vis diffuse-reflectance spectra were measured. As a result, **2-Cl** and **2-Br** displayed almost identical absorption edges to those of **1-Cl** and **1-Br** (Figure 2, dashed lines; see also Figure S4), indicating that $[PtCl_2(ppy)]^-$ and $[PtBr_2(ppy)]^-$ ions in **2-X** crystals should behave as "discrete" molecules without Pt···Pt electronic interactions, similar to **1-X** (Figure S1). Therefore, their electronic and excited state characteristics are independent of the type of cation. Time-dependent density functional theory (TDDFT) calculations revealed that the lowest-energy absorption bands are assignable to the monomer-based singlet metal-to-ligand charge transfer (^{1}MLCT) transition mixed with the singlet halide-to-ligand charge transfer (^{1}XLCT) transition, that is, ^{1}(M+X)LCT transition (Figure S5).

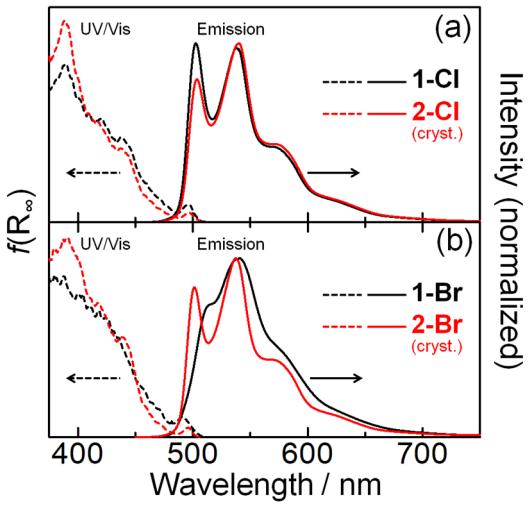

Figure 2. UV/Vis diffuse-reflectance spectra (dashed lines) and emission spectra (solid lines, λ_{ex} = 350 nm) of (a) **1-Cl** and **2-Cl**, and (b) **1-Br** and **2-Br** at 298 K in the crystal phase.

All the complexes exhibited green luminescence in their crystal phases at 298 K. The vibronically structured profiles of the spectra (Figure 2, solid lines) indicate the emission from the ligand-centered $^3\pi\pi^*$ excited state of the discrete molecules. The maxima of the first vibrational satellite band of **1-Cl** (503 nm, which is consistent with that in a previous report[12]) and **2-Cl** (504 nm) are almost comparable to that of **2-Br** (501 nm). Although the vibrational structure of **1-Br** was not so obvious, the high-energy edges of the emission band, as well as the maximum of the second vibrational satellite bands, were almost comparable (538 nm for **1-Cl**, 540 nm for **2-Cl**, 541 nm for **1-Br**, and 537 nm for **2-Br**), suggesting the similarity of the emission origins. Further, the emissions of **2-Cl** and **2-Br** disappeared in the supercooled liquid phases (Figures 3(b) and S6), in contrast to the liquid-phase luminescence behavior of $(C_2mim)[Pt(CN)_2(ptpy)]$ (C_2mim = 1-ethyll-3-methylimidazolium, *p*tpy = 2-(*p*-tolyl)pyridinate),[9] which is consistent with the emission quenching of **1-Cl** in solution.[12] This quenching is due to the weaker ligand field of Cl^- and Br^- compared with that of CN^-, which enhances the nonradiative deactivation through large structural deformation via the metal-centered ^{3}dd excited state.[18] Therefore, the present **2-Cl** and **2-Br** are unique systems that can adopt both the luminescent crystalline phase and the non-luminescent supercooled liquid phase at room temperature (Figure 3(a,b)). Below the glass transition point, the glasses of **2-Cl** and **2-Br** exhibited intense green $^3\pi\pi^*$ luminescence (Figures 3(c) and S7) because the increased rigidity of the glass phase should prevent structural deformation. The enhancement of the first vibrational satellite band of emission at 77 K (Figure 3(c)) also indicates less structural deformation.

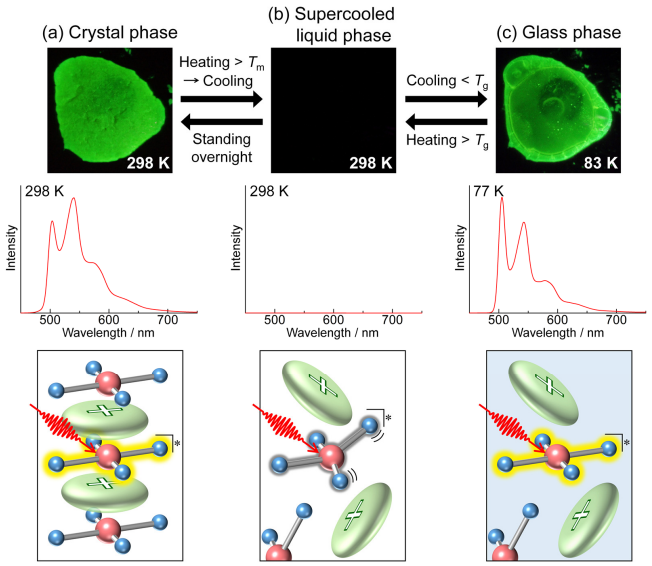

Figure 3. Photographs of **2-Cl** under UV irradiation (top), emission spectra of **2-Cl** (middle, λ_{ex} = 350 nm), and schematic representations of **2-Cl** and **2-Br** (bottom) at (a) crystal, (b) supercooled liquid, and (c) glass phases. Square-planar species and green ellipsoids denote $[PtX_2(ppy)]^-$ and $P_{6,6,6,14}$ ions, respectively.

The remarkable difference between the chloride and bromide complexes was in the emission intensity at 298 K. Photophysical parameters are listed in Table 2. At 298 K, high emission quantum yields (Φ) were observed for **1-Cl** (Φ = 0.49) and **2-Cl** (crystal, Φ = 0.40), whereas they decreased significantly for **1-Br** (Φ = 0.03) and **2-Br** (crystal, Φ = 0.04). At 77 K, however, the crystals of **1-Br** and **2-Br**, as well as the glass phases, exhibited high emission quantum yields comparable to those of **1-Cl** and **2-Cl**. Based on the emission quantum yields and emission lifetimes, the radiative and nonradiative rate constants (k_r and k_{nr}, respectively) were estimated to understand the photophysical processes. The determined k_r values, which reflect the radiative process, of all

complexes are in the range of 0.9–1.5 × 10^5 s^{-1} at 298 K, indicating the similarity of the luminescence origin between **1-X** and **2-X**. It should be noted that these k_r values are significantly larger than those of Pt(II) complexes showing "purer" ^{3}ππ* emissions (~10^4 s^{-1}; Chart S1(a)),[19-21] suggesting the perturbation of the ^{3}ππ* state by the ^{3}(M+X)LCT state (Chart S1(b)).[20a,21a] In addition, the larger k_{nr} values of **1-Br** and **2-Br** at 298 K than those of **1-Cl** and **2-Cl** suggested the presence of an additional thermally activated deactivation process through the nonradiative excited state, such as the metal-centered ^{3}dd state.[18,22]

Table 2. Photophysical parameters of complexes.[a]

	Phase	T / K	τ[b] / μs	Φ[c]	k_r[d] / s^{-1}	k_{nr}[e] / s^{-1}
1-Cl	Crystal	298	3.2	0.49	1.5 × 10^5	1.5 × 10^5
	Crystal	77	5.5	0.63	1.2 × 10^5	6.8 × 10^4
2-Cl	Crystal	298	3.1	0.40	1.3 × 10^5	1.9 × 10^5
	Crystal	77	6.4	0.71	1.1 × 10^5	4.5 × 10^4
	Liquid	298	–	–	–	–
	Glass	77	6.3	0.52	8.2 × 10^4	7.6 × 10^4
1-Br	Crystal	298	0.22	0.03	1.4 × 10^5	4.4 × 10^6
	Crystal	77	4.4	0.55	1.2 × 10^5	1.0 × 10^5
2-Br	Crystal	298	0.43	0.04	9.3 × 10^4	2.1 × 10^6
	Crystal	77	6.4	0.55	8.6 × 10^4	7.0 × 10^4
	Liquid	298	–	–	–	–
	Glass	77	4.9	0.34	6.9 × 10^4	1.3 × 10^5

[a] Detailed fitting results are presented in Table S1. [b] Emission lifetimes. [c] Emission quantum yield. [d] Radiative rate constants, $k_r = \Phi/\tau$. [e] Nonradiative rate constants $k_{nr} = k_r(1 - \Phi)/\Phi$.

To confirm the emission origins and the deactivation process, the temperature dependences of the emission lifetimes were investigated (Figure 4(a,b)). Among the present complexes, **1-Cl** and **1-Br** were selected for this purpose instead of **2-Cl** and **2-Br** because the Bu_4N^+ cation is known to play a role as a less-polar frozen solvent matrix suitable for photophysical analyses over a wide temperature range.[2d,19,20,23] The temperature dependence in the lower-temperature region (4–125 K) is mainly due to the zero-field splitting (ZFS) of the excited triplet sublevels, which reflect the degree of the contribution of heavy atoms (i.e., Pt) to the emission state. For example, the emission lifetimes of Pt(II) complexes showing "purer" ^{3}ππ* emission display only weak temperature dependence because of the very small ZFS values (< 2 cm^{-1}; Chart S2(a)).[19,20a,21a,c] If the ^{3}ππ* excited state is mixed with ^{3}MLCT (or ^{3}(M+X)LCT) states, the ZFS becomes larger (approx. 5–50 cm^{-1}; Chart S2(b)) owing to the spin-orbit coupling (SOC), causing the temperature dependence.[20a,21b] Because the emission spectral shapes were almost maintained in this temperature region (Figure S8), we have ruled out other possible origins of the temperature dependence. As shown in Figure 4(c,d), the ZFS values (energy separations between the lowest and highest sublevels) were estimated to be 129 and 104 cm^{-1} for **1-Cl** and **1-Br**, respectively, from the temperature dependence profile (see Experimental Section in the Supporting Information for details).[24] Importantly, these ZFS values were unexpectedly large compared to those of not only the "purer" ^{3}ππ* (< 2 cm^{-1}) but also the typical ^{3}ππ*/^{3}MLCT mixed (approx. 5–50 cm^{-1}) excited states of Pt(II) complexes,[1d,21a,25] and comparable to those of the ^{3}MLCT and related excited states (approx. 50–200 cm^{-1}; Chart S2(c,d)),[1d,26,27] revealing the unusually large contribution of the ^{3}(M+X)LCT character to the ^{3}ππ* state of the complexes. Such large ^{3}ππ*/^{3}(M+X)LCT mixing is further confirmed by the SOC-included DFT calculations for the T_1 state of the complexes (Figure S9), and this conclusion is also consistent with previous DFT results.[28] In the higher-temperature region (125–300 K), the emission lifetime of **1-Br** decreased significantly with increasing temperature, while the temperature dependence for **1-Cl** was small. The temperature dependence for **1-Br** at 125–300 K suggested the presence of thermally activated decay through the metal-centered ^{3}dd excited state, where the estimated decay rate constant from the ^{3}dd state (1.29 × 10^{10} s^{-1}; Figure S10) was a reasonable value.[20,21a,c,29] In contrast, less temperature dependence for **1-Cl** at 125–300 K indicated the suppression of deactivation through the ^{3}dd state. Because the k_{nr} values of **1-Cl** and **2-Cl** are comparable at 298 K (Table 2), the quenching of the excited state of **2-Cl** through the ^{3}dd state should be similarly suppressed, which enables the bright emission of **2-Cl** in the crystal phase. This difference in quenching could be due to the weaker ligand-field strength of Br^- compared with that of Cl^- (Figure S11).

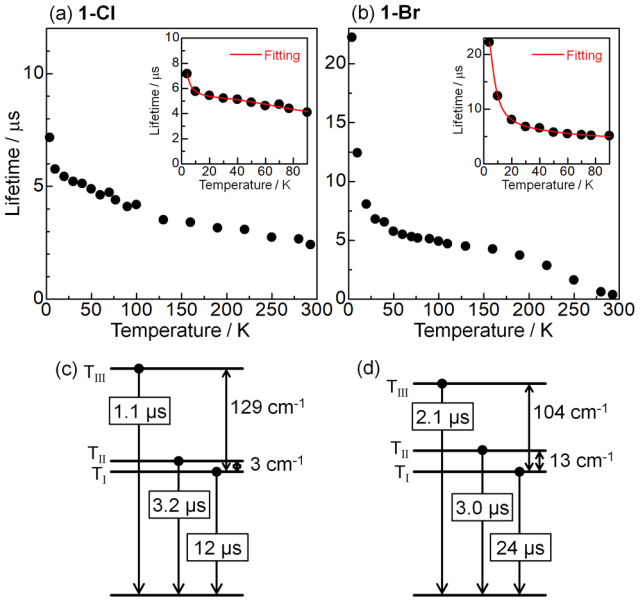

Figure 4. (a,b) Temperature dependence of emission lifetimes of (a) **1-Cl** and (b) **1-Br**. The red lines in the insets are the fitted curves the fitting results based on Eq. (1) in Experimental Section (Supporting Information). (c,d) Energy diagrams of the triplet spin sublevels of (c) **1-Cl** and (d) **1-Br** (details of fitting parameters are summarized in Table S2).

Overall, these photophysical studies revealed the highly contrasting luminescent behavior of **2-Cl** between the crystal and supercooled liquid phases: bright luminescence in the crystal phase and non-luminescence in the supercooled liquid phase. The bright luminescent behavior of **2-Cl** and **1-Cl** in the crystal phase originates from the enhancement of the k_r value and the suppression of the deactivation through the ^{3}dd state, where the former is due to the large mixing of the ^{3}(M+X)LCT character to

the $^3\pi\pi^*$ excited state. Such large $^3\pi\pi^*/^3$(M+X)LCT mixing could be due to the destabilization of the Pt 5d orbitals by conjugation with halide ligands (Figure S9). Although the radiative processes of **1-Br** and **2-Br** are similar to those of **1-Cl** and **2-Cl**, the relatively strong π-donation of the Br^- ligand quenched the emission of **1-Br** and **2-Br** at ambient temperature, resulting in their lower emission behavior. Because the excited state of $[PtCl_2(ppy)]^-$ completely quenched in fluid media,[12] the emission of **2-Cl** disappeared in the supercooled liquid phase, enabling the high-contrast luminescence ON/OFF switching between crystal and supercooled liquid phases triggered by external stimuli, as described in the next section.

Fabrication of Stimuli-responsive Film

The abovementioned thermal and photophysical behaviors of the present complexes allow the fabrication of a non-doped stimuli-responsive luminescent film of **2-Cl** through facile procedures. Typically, the powder sample of **2-Cl** was melted on a glass substrate and molded by pressing it gently between two glass plates or spread manually using a spatula. After standing at room temperature (298 K), the melted **2-Cl** slowly crystallized to form a polycrystalline film (hereafter named as **2-Cl-film**) while maintaining the translucency (inset of Figure 5(a); see also Figure S12). The X-ray diffraction pattern of the **2-Cl-film** clearly showed sharp peaks similar to those of the **2-Cl** powder (Figure 5(a)), but fewer peaks for the **2-Cl-film** indicated the anisotropic crystal growth on the glass substrate. Indeed, the scanning electron microscopy (SEM) observations clearly showed the anisotropic orientation of very thin crystals (width of approx. 2 μm; Figures 5(b) and S13) owing to the radial growth from the nucleation center. The presence of radial crystal growth domains was also confirmed by polarized optical microscopy (Figure S14). The resulting **2-Cl-film** displayed brilliant green emission with CIE coordinates of (0.32, 0.62) (Figures 5(c) and S15). Such translucent films should have advantages for various applications, including optical and optoelectronic devices.

The **2-Cl-film** exhibited thermally and mechanically induced ON/OFF luminescence. As shown in Figure 5(c), the emission of the **2-Cl-film** disappeared above the melting point (326 K; Figure S16) and was not restored immediately after cooling to 298 K, while it was recovered by standing at 298 K overnight. This thermal luminescence ON/OFF cycle could be repeated without degradation (Figure S17), enabling high-contrast ON/OFF switching with high reproducibility. Although such crystallization-induced luminescence of ionic liquids has also been reported previously,[30] in the present system, mechanical stimuli such as scratching drastically accelerated the crystallization of the metastable supercooled ionic liquid phase of **2-Cl** at ambient temperature. As shown in Figure 6(a), the bright luminescent crystals of **2-Cl** grew radially from the supercooled liquid phase of the **2-Cl-film** after the pinpoint mechanostress (see also Supplementary Movie). Because such radial crystal growth was also observed in the thermal crystallization (Figures S12–S13), the nucleation by mechanostress should accelerate the crystallization. As a result, the apparent quantum yield reached Φ ~ 0.05 (observable by the naked eye), within 25 min after the mechanostress, while the recovery to Φ ~ 0.05 requires 150 min without mechanical initiation (Figure 6(b)). By applying this mechanically triggered luminescence behavior, we realized mechanical writing on the melted **2-Cl-film** and erasure by heating (Figure 6(c)). Overall, the co-existence of the cold crystallization behavior and the crystallization-induced luminescence behavior of **2-Cl** enabled us to fabricate a high-contrast luminescence ON/OFF switchable thin film triggered by mechanostress.

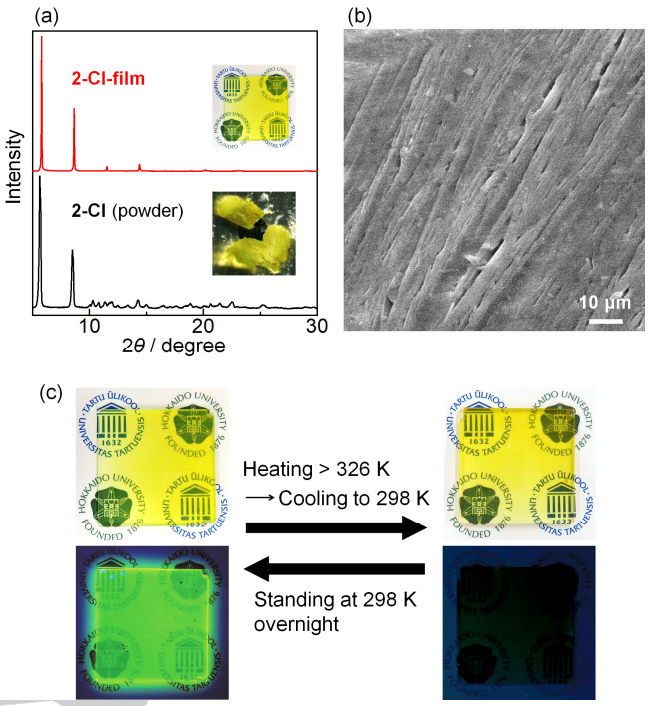

Figure 5. (a) PXRD patterns of **2-Cl** powder (black) and **2-Cl-film** (red). (b) SEM image of the **2-Cl-film**. (c) Photographs showing thermal ON/OFF switching of the luminescence of the **2-Cl-film** under bright field (top) and UV light (bottom).

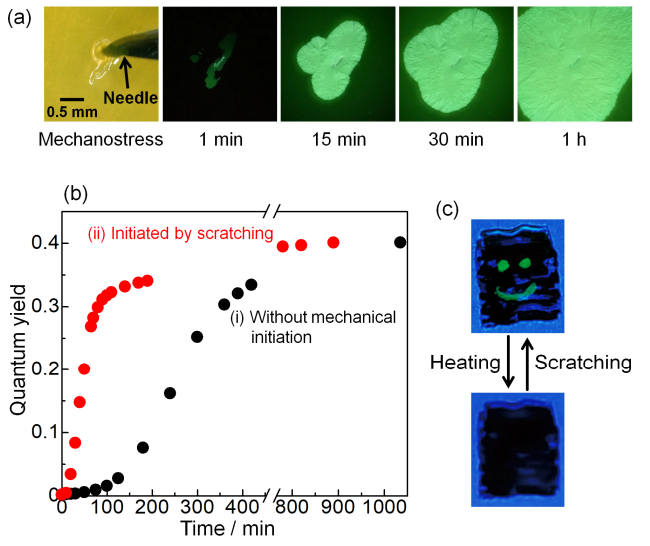

Figure 6. (a) Photographs of progression of the crystallization of the melted **2-Cl-film** (fabricated by the spin-coating (8,000 rpm, 60 s)) triggered by a pinpoint mechanostress. (b) Time-course of the apparent emission quantum yield of the **2-Cl-film** (λ_{ex} = 388 nm) at 298 K (i) in the absence of mechanostress or (ii) initiated by scratching by spatula after melting. (c) Photographs of the melted **2-Cl-film** before and after scratching by spatula.

Conclusion

In conclusion, we have succeeded in the synthesis of the liquescent Pt(II) complex **2-Cl**, showing obvious phosphorescence ON/OFF switching coupled with the phase transition at ambient temperature. The complexes **2-Cl** and **2-Br** showed bi-stability between the crystal and supercooled liquid phases even at ambient temperature. In particular, **2-Cl** exhibited bright luminescence in the crystal phase due to the large mixing of the ^{3}(M+X)LCT character with the $^3\pi\pi^*$ emission, as evidenced by the large ZFS value, as well as the suppression of the quenching through the ^{3}dd state. Because this bright $^3\pi\pi^*/^3$(M+X)LCT phosphorescence in the crystal phase is drastically quenched in the liquid phase, **2-Cl** enables stimuli-triggered high-contrast luminescence ON/OFF switching. Based on the present system, a mechanostress-responsive translucent thin film was successfully fabricated. The present system is unique as the first system that exhibits luminescence change coupled with the phase transition from the supercooled liquid state of transition-metal complexes by external stimuli. In addition, although the luminescence of the $[PtCl_2(ppy)]^-$ anion itself was reported very early,[12] the photophysical studies has not been conducted in detail, because it was mainly used as a starting material to construct the complexes with stronger ligand fields (e.g., CN^- or alkynyl).[2] The unusually large contribution of the ^{3}(M+X)LCT character to the $^3\pi\pi^*$ luminescence was revealed in this study. We believe that the present study will offer new perspectives not only for easily fabricated luminescent optical devices with large surface areas but also for the development of rewritable optical papers driven by mechanical stimuli and thermal treatment. Further studies of luminescent Pt(II)-complex ionic liquids are in progress toward applications in optical devices and sensors.

Acknowledgements

This work was supported by JSPS KAKENHI, grant numbers JP17H06367, JP18K19086, JP18K14232, and JP21K05094, and the University of Tartu Foundation. The authors are grateful to Prof. S. Takeda, Dr. Y. Kageyama, and Mr. R. Mizoue (Hokkaido Univ.) for the support regarding DSC measurements, and Dr. A. Matsumoto (Hokkaido Univ.) for the support regarding SEM observations. Supercomputing resources at the Research Center for Computational Science, Okazaki, Japan are also acknowledged.

Conflict of interest

The authors declare no conflict of interest.

Keywords: cyclometalating ligand • ionic liquid • mechanoresponse • photophysics • platinum complex

[1] a) R. C. Evans, P. Douglas, C. J. Winscom, *Coord. Chem. Rev.* **2006**, *250*, 2093–2126; b) J. A. G. Williams, S. Develay, D. L. Rochester, L. Murphy, *Coord. Chem. Rev.* **2008**, *252*, 2596–2611; c) W.-Y. Wong, C.-L. Ho, *Coord. Chem. Rev.* **2009**, *253*, 1709–1758; d) H. Yersin, A. F. Rausch, R. Czerwieniec, T. Hofbeck, T. Fischer, *Coord. Chem. Rev.* **2011**, *255*, 2622–2652; e) V. W.-W. Yam, K. M.-C. Wong, *Chem. Commun.* **2011**, *47*, 11579–11592; f) J. Wang, F. Zhang, J. Zhang, W. Tang, A. Tang, H. Peng, Z. Xu, F. Teng, Y. Wang, *J. Photochem. Photobiol. C* **2013**, *17*, 69–104; g) V. W.-W. Yam, A. S.-Y. Law, *Coord. Chem. Rev.* **2020**, *414*, 213298.

[2] a) Y. Chi, P.-T. Chou, *Chem. Soc. Rev.* **2010**, *39*, 638–655; b) S. Huo, J. Carroll, D. A. K. Vezzu, *Asian J. Org. Chem.* **2015**, *4*, 1210–1245; c) K. Li, G. S. M. Tong, Q. Wan, G. Cheng, W.-Y. Tong, W.-H. Ang, W.-L. Kwong, C.-M. Che, *Chem. Sci.* **2016**, *7*, 1653–1673; d) M. Yoshida, M. Kato, *Coord. Chem. Rev.* **2020**, *408*, 213194.

[3] a) M. Kato, *Bull. Chem. Soc. Jpn.* **2007**, *80*, 287–294; b) O. S. Wenger, *Chem. Rev.* **2013**, *113*, 3686–3733; c) Q. Zhao, F. Li, C. Huang, *Chem. Soc. Rev.* **2010**, *39*, 3007–3030; d) X. Zhang, B. Li, Z.-H. Chen, Z.-N. Chen, *J. Mater. Chem.* **2012**, *22*, 11427–11441; e) A. Kobayashi, M. Kato, *Eur. J. Inorg. Chem.* **2014**, 4469–4483; f) V. W.-W. Yam, V. K.-M. Au, S. Y.-L. Leung, *Chem. Rev.* **2015**, *115*, 7589–7728; g) A. Aliprandi, D. Genovese, M. Mauro, L. De Cola, *Chem. Lett.* **2015**, *44*, 1152–1169; h) M. Kato, H. Ito, M. Hasegawa, K. Ishii, *Chem. Eur. J.* **2019**, *25*, 5105–5112; i) M. A. Soto, R. Kandel, M. J. MacLachlan, *Eur. J. Inorg. Chem.* **2021**, 894–906.

[4] For example: a) P. Brulatti, V. Fattori, S. Muzzioli, S. Stagni, P. P. Mazzeo, D. Braga, L. Maini, S. Militae, M. Cocchi, *J. Mater. Chem. C* **2013**, *1*, 1823–1831; b) W.-C. Chen, C. Sukpattanacharoen, W.-H. Chan, C.-C. Huang, H.-F. Hsu, D. Shen, W.-Y. Hung, N. Kungwan, D. Escudero, C.-S. Lee, Y. Chi, *Adv. Funct. Mater.* **2020**, *30*, 2002494; c) J.-J. Wang, C. Chen, W.-G. Chen, J.-S. Yao, J.-N. Yang, K.-H. Wang, Y.-C. Yin, M.-M. Yao, L.-Z. Feng, C. Ma, F.-J. Fan, H.-B. Yao, *J. Am. Chem. Soc.* **2020**, *142*, 3686−3690.

[5] For example: a) C. S. Smith, K. R. Mann, *J. Am. Chem. Soc.* **2012**, *134*, 8786−8789; b) M. M. Suárez, B. F. E. Curchod, I. Tavernelli, U. Rothlisberger, R. Scopelliti, I. Jung, D. D. Censo, M. Grätzel, J. F. F. Sánchez, A. F. Gutiérrez, M. K. Nazeeruddin, E. Baranoff, *Chem. Mater.* **2012**, *24*, 2330−2338; c) M. J. Bryant, J. M. Skelton, L. E. Hatcher, C. Stubbs, E. Madrid, A. R. Pallipurath, L. H. Thomas, C. H. Woodall, J. Christensen, S. Fuertes, T. P. Robinson, C. M. Beavers, S. J. Teat, M. R. Warren, F. Pradaux-Caggiano, A. Walsh, F. Marken, D. R. Carbery, S. C. Parker, N. B. McKeown, R. Malpass-Evans, M. Carta, P. R. Raithby, *Nat. Commun.* **2017**, *8*, 1800; d) Y. Li, L. Chen, Y. Ai, E. Y.-H. Hong, A. K.-W. Chan, V. W.-W. Yam, *J. Am. Chem. Soc.* **2017**, *139*, 13858−13866.

[6] a) A. Sandström, A. Asadpoordarvish, J. Enevold, L. Edman, *Adv. Mater.* **2014**, *26*, 4975–4980; b) F. Lu, T. Nakanishi, *Adv. Opt. Mater.* **2019**, *7*, 1900176; c) D. Zhang, S. Suzuki, T. Naota, *Angew. Chem. Int. Ed.* **2021**, *60*, 19701–19704.

[7] For example: a) S. Arenz, A. Babai, K. Binnemans, K. Driesen, R. Giernoth, A.-V. Mudring, P. Nockemann, *Chem. Phys. Lett.* **2005**, *402*, 75–79; b) S. Tang, A. Babai, A.-V. Mudring, *Angew. Chem. Int. Ed.* **2008**, *47*, 7631–7634; c) B. Mallick, B. Balke, C. Felser, A.-V. Mudring, *Angew. Chem. Int. Ed.* **2008**, *47*, 7635–7638; d) H. Li, H. Shao, Y. Wang, D. Qin, B. Liu, W. Zhang, W. Yan, *Chem. Commun.* **2008**, 5209–5211; e) K. Lunstroot, P. Nockemann, K. Van Hecke, L. Van Meervelt, C. Görller-Walrand, K. Binnemans, K. Driesen, *Inorg. Chem.* **2009**, *48*, 3018–3026; f) K. Pohako-Esko, T. Wehner, P. S. Schulz, F. W. Heinemann, K. Müller-Buschbaum, P. Wasserscheid, *Eur. J. Inorg. Chem.* **2016**, 1333–1339; g) J. Alvarez-Vicente, S. Dandil, D. Banerjee, H. Q. N. Gunaratne, S. Gray, S. Felton, G. Srinivasan, A. M. Kaczmarek, R. Van Deun, P. Nockemann, *J. Phys. Chem. B* **2016**, *120*, 5301–5311; h) K.-L. Cheng, W.-L. Yuan, L. He, N. Tang, H.-M. Jian, Y. Zhao, S. Qin, G.-H. Tao, *Inorg. Chem.* **2018**, *57*, 6376–6390; i) T. Iimori, H. Sugawa, N. Uchida, *J. Phys. Chem. B* **2020**, *124*, 8317–8322.

[8] For example: a) Y. Yoshida, J. Fujii, G. Saito, T. Hiramatsu, N. Sato, *J. Mater. Chem.* **2006**, *16*, 724–727; b) S. Pitula, A.-V. Mudring, *Chem. Eur. J.* **2010**, *16*, 3355–3365; c) A. Tokarev, J. Larionova, Y. Guari, J. M. López-de-Luzuriaga, M. Monge, P. Dieudonné, C. Blanc, *Dalton Trans.* **2010**, *39*, 10574–10576; d) S. Gago, L. Cabrita, J. C. Lima, L. C. Branco, F. Pina, *Dalton Trans.* **2013**, *42*, 6213–6218; e) E. T. Spielberg, E. Edengeiser, B. Mallick, M. Havenith, A.-V. Mudring, *Chem. Eur. J.* **2014**, *20*, 5338–5345; f) T. Tominaga, T. Mochida, *Chem. Eur. J.* **2018**, *24*, 6239–6247; g) T. Narita, K. Fujii, T. Endo, Y. Kimura, *J. Mol. Liq.* **2020**, *318*, 114212; h) S.-Y. Cho, T. Mochida, *Chem. Lett.* **2021**, *50*, 1740–1742.

[9] a) T. Ogawa, M. Yoshida, H. Ohara, A. Kobayashi, M. Kato, *Chem. Commun.* **2015**, *51*, 13377–13380; b) T. Ogawa, W. M. C. Sameera, M. Yoshida, A. Kobayashi, M. Kato, *Dalton Trans.* **2018**, *47*, 5589–5594.

[10] S. Suzuki, D. Yamaguchi, Y. Uchida, T. Naota, *Angew. Chem. Int. Ed.* **2021**, *60*, 8284–8288.

[11] C. C. L. Pereira, S. Dias, I. Coutinho, J. P. Leal, L. C. Branco, C. A. T. Laia, *Inorg. Chem.* **2013**, *52*, 3755−3764.

[12] a) C. J. Craig, F. O. Garces, R. J. Watts, R. Palmans, A. J. Frank, *Coord. Chem. Rev.* **1990**, *97*, 193–208; b) P.-I. Kvam, M. V. Puzyk, K. P. Balashev, J. Songstad, *Acta Chem. Scand.* **1995**, *49*, 335–343.

[13] J. J. Hu, S.-Q. Bai, H. H. Yeh, D. J. Young, Y. Chi, T. S. A. Hor, *Dalton Trans.* **2011**, *40*, 4402–4406.

[14] M. M. Mdleleni, J. S. Bridgewater, R. J. Watts, P. C. Ford, *Inorg. Chem.* **1995**, *34*, 2334–2342.

[15] P.-I. Kvam, T. Engebretsen, K. Maartmann-Moe, J. Songstad, *Acta Chem. Scand.* **1996**, *50*, 107–113.

[16] Y. Funasako, T. Mochida, K. Takahashi, T. Sakurai, H. Ohta, *Chem. Eur. J.* **2012**, *18*, 11929–11936.

[17] P.-I. Kvam, J. Songstad, *Acta Chem. Scand.* **1995**, *49*, 313–324.

[18] a) G. S.-M. Tong, C.-M. Che, *Chem. Eur. J.* **2009**, *15*, 7225–7237; b) Y. Luo, Y. Xu, W. Zhang, W. Li, M. Li, R. He, W. Shen, *J. Phys. Chem. C* **2016**, *120*, 3462–3471; c) R. Inoue, M. Naito, M. Ehara, T. Naota, *Chem. Eur. J.* **2019**, *25*, 3650–3661; d) P. Pinter, T. Strassner, *Chem. Eur. J.* **2019**, *25*, 4202–4205.

[19] A. F. Rausch, U. V. Monkowius, M. Zabel, H. Yersin, *Inorg. Chem.* **2010**, *49*, 7818–7825.

[20] a) T. Ogawa, W. M. C. Sameera, D. Saito, M. Yoshida, A. Kobayashi, M. Kato, *Inorg. Chem.* **2018**, *57*, 14086–14096; b) C. Wakasugi, M. Yoshida, W. M. C. Sameera, Y. Shigeta, A. Kobayashi, M. Kato, *Chem. Eur. J.* **2020**, *26*, 5449–5458.

[21] a) A. Bossi, A. F. Rausch, M. J. Leitl, R. Czerwieniec, M. T. Whited, P. I. Djurovich, H. Yersin, M. E. Thompson, *Inorg. Chem.* **2013**, *52*, 12403–12415; b) H. Uesugi, T. Tsukuda, K. Takao, T. Tsubomura, *Dalton Trans.* **2013**, *42*, 7396–7403; c) A. M. Prokhorov, T. Hofbeck, R. Czerwieniec, A. F. Suleymanova, D. N. Kozhevnikov, H. Yersin, *J. Am. Chem. Soc.* **2014**, *136*, 9637–9642.

[22] a) J. A. G. Willams, *Top. Curr. Chem.* **2007**, *281*, 205–268; b) A. Ito, T. J. Meyer, *Phys. Chem. Chem. Phys.* **2012**, *14*, 13731–13745; c) T. Sajoto, P. I. Djurovich, A. B. Tamayo, J. Oxgaard, W. A. Goddard III, M. E. Thompson, *J. Am. Chem. Soc.* **2009**, *131*, 9813–9822.

[23] a) L. Ricciardi, M. La Deda, A. Ionescu, N. Godbert, I. Aiello, M. Ghedini, *Dalton Trans.* **2017**, *46*, 12625–12635; b) A. Ionescu, N. Godbert, I. Aiello, L. Ricciardi, M. La Deda, A. Crispini, E. Sicilia, M. Ghedini, *Dalton Trans.* **2018**, *47*, 11645–11657.

[24] G. D. Hager, G. A. Crosby, *J. Am. Chem. Soc.* **1975**, *97*, 7031−7037.

[25] H. Yersin, J. Strasser, *Coord. Chem. Rev.* **2000**, *208*, 331–364.

[26] D. Saito, T. Ogawa, M. Yoshida, J. Takayama, S. Hiura, A. Murayama, A. Kobayashi, M. Kato, *Angew. Chem. Int. Ed.* **2020**, *59*, 18723–18730.

[27] J. C. Deaton, A. Chakraborty, R. Czerwieniec, H. Yersin, F. N. Castellano, *Phys. Chem. Chem. Phys.* **2018**, *20*, 25096–25104.

[28] C. Gourlaouen, C. Daniel, *Dalton Trans.* **2014**, *53*, 17806–17819.

[29] a) C. B. Blanton, Z. Murtaza, R. J. Shaver, D. P. Rillema, *Inorg. Chem.* **1992**, *31*, 3230–3235; b) A. F. Rausch, L. Murphy, J. A. G. Williams, H. Yersin, *Inorg. Chem.* **2012**, *51*, 312–319.

[30] a) Z.-P. Wang, J.-Y. Wang, J.-R. Li, M.-L. Feng, G.-D. Zou, X.-Y. Huang, *Chem. Commun.* **2015**, *51*, 3094–3097; b) N. Shen, J. Li, Z. Wu, B. Hu, C. Cheng, Z. Wang, L. Gong, X. Huang, *Chem. Eur. J.* **2017**, 23, 15795–15804.

Entry for the Table of Contents

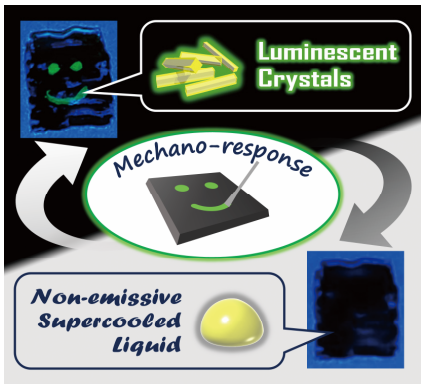

Photofunctional thin film with supercooled liquid/crystal bi-stability has been fabricated using a trihexyltetradecylphosphonium salt of a luminescent Pt(II) complex with a low melting point. Since the emission of the complex changed significantly between the crystal and the supercooled liquid phases, this thin film could switch luminescence ON/OFF through crystallization by mechanostress and melting by gentle heating.